

## A Gain Enhanced Multiband Antenna using SRRs with Defected Ground Structure

Diptiranjan Samantaray<sup>(1)</sup>, Somak Bhattacharyya<sup>(2)</sup> and K. V. Srinivas<sup>(3)</sup>

Department of Electronics Engineering, Indian Institute of Technology (BHU), Varanasi, India

<sup>(1)</sup>[drsamantaray.rs.ece17@iitbhu.ac.in](mailto:drsamantaray.rs.ece17@iitbhu.ac.in), <sup>(2)</sup>[somakbhattacharyya.ece@iitbhu.ac.in](mailto:somakbhattacharyya.ece@iitbhu.ac.in), <sup>(3)</sup>[kvsrinivas.ece@iitbhu.ac.in](mailto:kvsrinivas.ece@iitbhu.ac.in)

### Abstract

The performance of tapered shaped octagonal patch antenna embedded with split ring resonators (SRRs) in its square slots along with defected ground has been analyzed in this paper for multiband frequency applications. The designed antenna operates over three distinct frequencies viz., 3.31 GHz, 6.50 GHz and 12.01GHz with the respective fractional bandwidths of 19.6%, 8.6% and 29.8%. The maximum return loss of -57 dB has been achieved over the band 10.36-13.95 GHz while the maximum realized gain of 22 dB has been obtained at 12.07 GHz. The antenna exhibits endfire radiation pattern in its far-field characteristics. The proposed antenna finds its applications in defense and military, satellite communication, several medical applications like cancerous cell detection, tumor and microimaging in medical analysis for determination of radio waves and also in many communication fields.

### 1. Introduction

The electromagnetics properties of the medium like effective permittivity, permeability or both can be negative for some frequencies due to the resonant behavior of unit cells in a metamaterial [1]. A combination of periodically arranged split ring resonators (SRRs) and thin wire have been used to realize simultaneously negative effective permittivity as well as permeability over a frequency regime [2, 3]. Later, researchers have replaced the thin wires with metallic plates in the bottom and the SRRs with different modifications on the top of the dielectric substrate [3, 4]. Other kinds of structures apart from SRRs have also been exploited by the research communities to enhance the desired electromagnetic properties of a medium [2-5]. Thus the metamaterial based structures have continued to attract the researchers for new applications in the field of microwave and higher frequency bands such as absorber, polarizer, subwavelength focusing, cloaking, lensing and improved metasurface antennas, filters etc. [1-6]. Recently, metamaterial based antenna and its feed system in wireless communications demand multi-functionalities such as flexibility and feasibility, ease of fabrication and integration, low profile, inexpensive and wideband or multiband operating with enhanced gain [2-6]. Owing to all these facts, metamaterial-based antennas have been

emerged for compact design with miniaturized geometrical shape having high gain or directivity [3-5].

SRRs based tapered patch antenna with defected ground structure has been implemented in this paper. Generally, a single SRR structure behaves as a simple RLC resonator with a few constructive and destructive couplings [4-6]. To reduce the ohmic loss and thereby to increase gain, the SRRs have been incorporated within the patch.

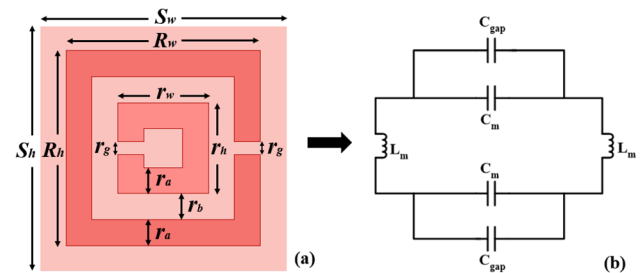


**Figure 1.** (a) Double ring square split ring resonator (SRR) structure (Designed parameters  $S_h = 4\text{mm}$ ,  $S_w = 4\text{mm}$ ,  $R_h = 3\text{mm}$ ,  $R_w = 3\text{mm}$ ,  $r_h = 1.4\text{mm}$ ,  $r_w = 1.4\text{mm}$ ,  $r_a = 0.4\text{mm}$ ,  $r_b = 0.4\text{mm}$ ,  $r_g = 0.2\text{mm}$ ) and its (b) equivalent RLC resonator circuit [6].

A single SRR structure along with its equivalent circuit model is represented in Figure 1(a) and Figure 1(b) respectively. The resonant frequency is obtained by using the equivalent circuit analysis method [5, 6]. The resonant frequency  $f_0$  of the square SRR is given in (1).

$$f_0 = \frac{1}{2\pi} \frac{1}{\sqrt{L_m(C_m + C_{gap})}} \approx \frac{1}{2\pi} \frac{1}{\sqrt{L_m C_m}} \quad (1)$$

Here the inductance  $L_m$  and capacitance  $C_m$  are represented in (2) and (3) respectively where in (1),  $C_{gap}$  is the capacitance due to slot in the ring and  $A$  is the balance constant represented in (3).

$$L_m = \frac{\mu_0 r_b}{r_a} [R_w + r_w] \quad (2)$$

$$C_m = \frac{A \epsilon_0 \epsilon_r r_a (2R_w + 2r_w - r_g)}{2r_b} \quad (3)$$

In the proposed design of the antenna, four identical SRRs have been embedded in four different rectangular slots made in the top rectangular patch of a microstrip

antenna. Further to enhance the gain, the defected ground structure is used by involving rectangular slots [7]. The proposed antenna is designed to operate over three different frequencies viz., 3.31 GHz, 6.50 GHz and 12.01 GHz with fractional bandwidths of 19.6%, 8.6% and 29.89% respectively. The evolution of the final design of the proposed antenna has been discussed. The structure offers very good impedance matching at 12.01 GHz with a return loss of -57 dB while the maximum realized gain of 22 dB has been obtained at 12.07 GHz. The proposed antenna exhibits endfire radiation pattern in its far-field characteristics.

## 2. Design of SRRs Based Tapered Antenna

The proposed antenna consists of four SRRs on the four different rectangular slots on the patch of a simple microstrip antenna where the defected ground has been introduced using rectangular slots. The geometrical dimensions of all the four SRRs embedded into four different rectangular slots in the top metallic patch are made equal. The top and bottom views of the proposed antenna are shown in Figure 2(a) and Figure 2(b) respectively. The proposed antenna has been designed on FR-4 dielectric (relative permittivity of 4.4 and loss tangent of 0.025) with thickness 1.6 mm. All the optimized geometrical dimensions of proposed antenna are mentioned in Figure 2.

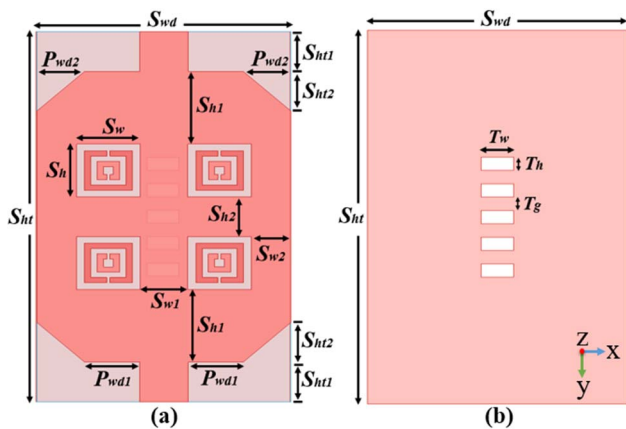


**Figure 2.** (a) Top view and (b) bottom view of the proposed antenna with enhanced gain (Designed parameters  $S_{wd} = 16$  mm,  $S_{ht} = 28$  mm,  $S_w = 4$  mm,  $S_h = 4$  mm,  $S_{ht1} = 3$  mm,  $S_{ht2} = 3$  mm,  $P_{wd1} = 3.47055$  mm,  $P_{wd2} = 3$  mm,  $S_{h1} = 5.5$  mm,  $S_{h2} = 3$  mm,  $S_{w1} = 3$  mm,  $S_{w2} = 2.5$  mm,  $T_w = 2$  mm,  $T_h = 1$  mm,  $T_g = 1$  mm).

The design of the proposed antenna has been obtained by optimizing a number of stages as shown in Figure 3. A rectangular patch with a dimension of  $22 \times 16$  mm<sup>2</sup> is sandwiched with a 28 mm long transmission line which is depicted in CASE-I of Figure 3. The maximum realized gain of 2.02 dB is observed at frequency of 13.65 GHz while the maximum fractional bandwidth of 14.19% at 10.78 GHz operating frequency has been observed. Later, the rectangular patch shape has been modified to octagonal shape which improves the fractional bandwidth to 16.9%

at 10.40 GHz operating frequency as represented in CASE-II of Figure 3. Now the defected ground concept is applied in CASE-III of Figure 3 to increase the realized gain to 7.1 dB at 12.2 GHz. Here five periodic  $2 \times 1$  mm<sup>2</sup> rectangular slots are incorporated in the ground which also enhances the fractional bandwidth to 31.25% at the operating frequency of 10.4 GHz.

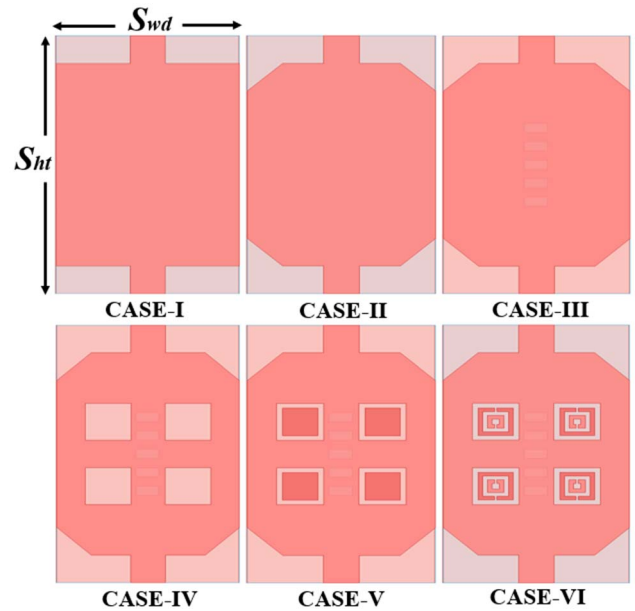


**Figure 3.** Design evolution for the proposed antenna with different modifications.

Next, four  $4 \times 4$  mm<sup>2</sup> rectangular slots have been introduced on top patch of the antenna which depicted in CASE-IV of Figure 3. Here the realized gain is 3.59 dB at 13.95 GHz along with the fractional bandwidth of 29.7% at 12.02 GHz. In CASE-V of Figure 3, again  $3 \times 3$  mm<sup>2</sup> square patch is incorporated at the top centre of four rectangular slots. It is clearly observed that the introduction of square patches has not affected the fractional bandwidth and realized gain of the antenna. So square shaped SRRs are added in place of square patch to enhance the gain by increasing the capacitance and inductance value which is shown in CASE-VI of Figure 3. The realized gain of 22 dB has been achieved at frequency of 12.07 GHz with 29.89% fractional bandwidth at 12.01 GHz operating frequency. This CASE-VI of Figure 3 is the final design of the proposed antenna due to improved performance.

## 3. Simulated Results

All the antennas shown in Figure 3 are simulated using Ansys HFSS and the respective return loss responses with respect to the frequency is shown in Figure 4. The proposed antenna mentioned in Figure 2 operates at three different frequencies viz., 3.31 GHz, 6.50 GHz and 12.01 GHz with fractional bandwidths of 19.6%, 8.6% and 29.8% respectively as shown in Figure 4. This antenna offers very good impedance matching at 12.01 GHz with a return loss of -57 dB. It is observed that the introduction of SRRs on

the patch improves the bandwidth along with the gain partially covering X and Ku-bands.

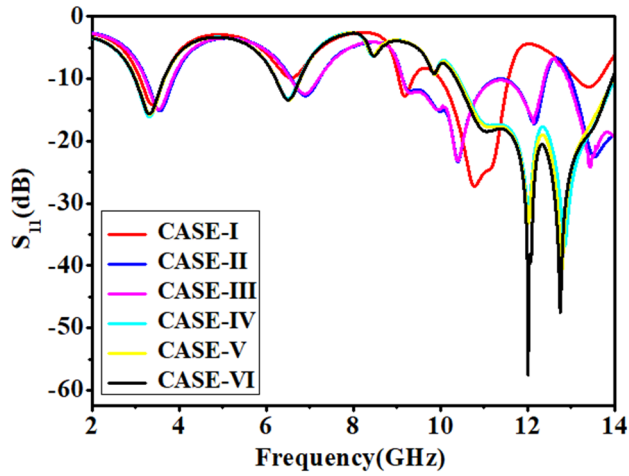


**Figure 4.** Plot of  $S_{11}$  (dB) with respect to frequency for different variations of antenna mentioned in Figure 3 along with the proposed antenna depicted in CASE-VI.

The electric field distributions at the top surface of the metallic patch without any inclusion of SRR together with the inclusion of SRRs have been shown in Figure 5(a) and Figure 5(b) respectively. The distributions of the electric field in the defected ground plane has also been studied and shown in Figure 5(c). It is also observed that they are maximum around the antenna aperture corresponding to the operating frequencies of 11.8 GHz, 12.07 GHz and 13.95 GHz. The maximum field distribution has been observed at 12.07 GHz due to combined inductive and capacitive effects of SRRs.

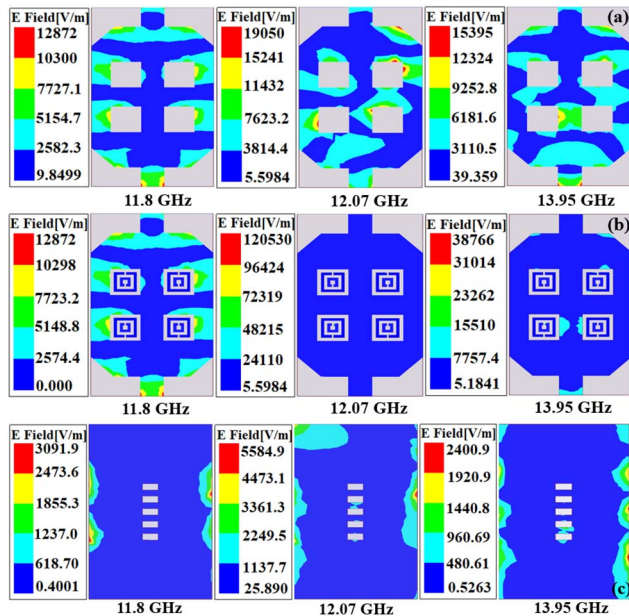


**Figure 5.** Simulated result of electric field distribution of proposed antenna at different operating frequencies.

The surface current distributions of the proposed antenna is also studied and shown in Figure 6. The surface current distribution at the top surface of the proposed antenna

without and with SRRs are represented in Figure 6(a) and Figure 6(b) respectively while the surface current distribution at the bottom surface is represented in Figure 6(c). They are more denser around the antenna aperture corresponding to the operating frequencies of 11.8 GHz, 12.07 GHz and 13.95 GHz. The surface current is maximum at 12.07 GHz to realize the best impedance matching.

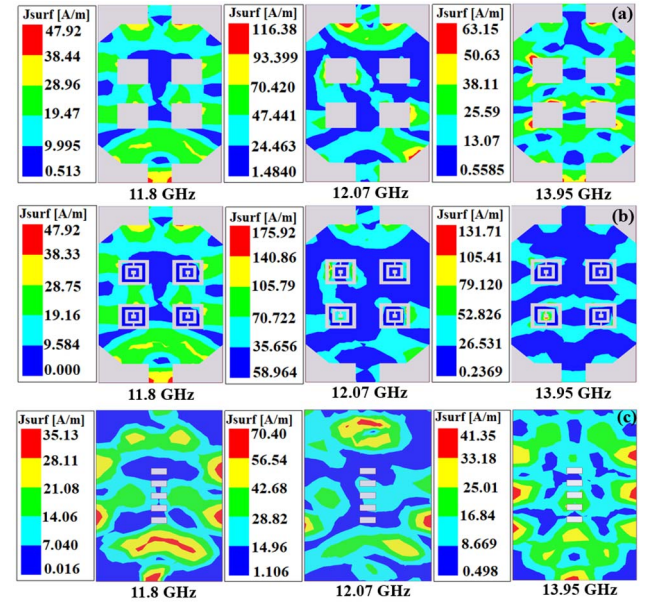


**Figure 6.** Simulated result of surface current of proposed antenna at different operating frequencies.

The three dimensional polar plot at different frequencies viz., 3.31 GHz, 6.51 GHz, 11.8 GHz, 12.07 GHz, 12.1 GHz and 13.95 GHz are shown in Figure 7. It is observed that the proposed antenna exhibits the realized gain of -7.04 dB, -3.76 dB, 5.01 dB, 22.02 dB, 21.27 dB and 3.33 dB at the respective operating frequencies. The realized gain is high over a band from 11.9 GHz to 12.2 GHz and the maximum gain of 22.02 dB has been achieved at 12.07 GHz.

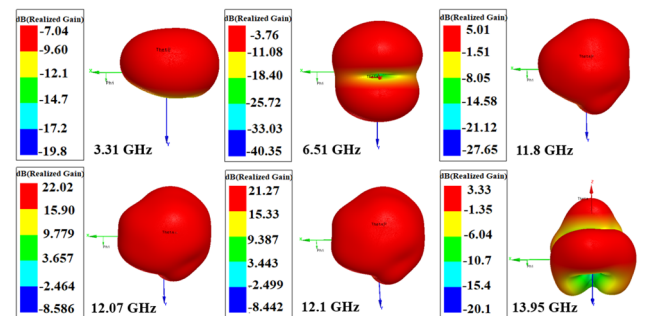


**Figure 7.** Simulated result of 3D realized gain polar plot of proposed antenna at different operating frequencies.

The E-plane ( $\varphi = 0^\circ$ ) and H-plane ( $\varphi = 90^\circ$ ) radiation characteristics of the proposed antenna at the operating frequencies of 11.8 GHz, 12.07 GHz and 13.95 GHz has been studied and shown in Figure 8(a) and Figure 8(b) respectively. Endfire radiation characteristics are observed at corresponding operating frequencies along E-plane

while nearly omnidirectional pattern is observed along H-plane. The cross-polarized level is found to be -15 dB below than the co-polarized level at all the operating frequencies as evident from Figure 8.

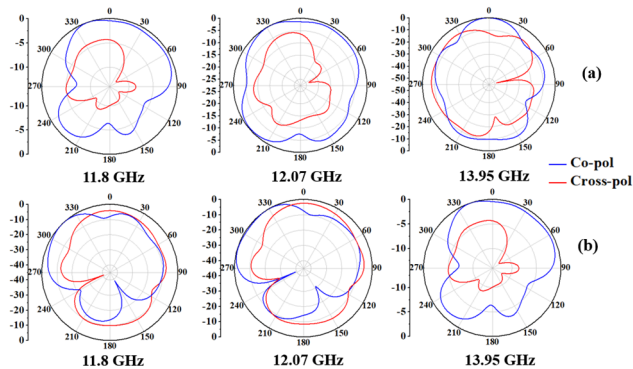


**Figure 8.** Co-polarized and Cross-polarized (a) E-plane and (b) H-plane at different operating frequencies within the proposed structure.

The proposed structure has been compared with the existing reported antenna structures as shown in Table 1. It is observed that the proposed design exhibits optimum fractional bandwidth and significant gain enhancement in comparison to the reported ones.

**Table 1.** Comparison of Proposed Antenna with Existing Antennas

Antenna Design	Dimension (mm <sup>2</sup> )	Fractional Bandwidth (%)	Gain (dB)
Joubert <i>et al.</i> [8]	125 x 125	4	10
Deng <i>et al.</i> [9]	45 x 45	20.8	2.8
Pan <i>et al.</i> [10]	27 x 27	6.9	3.1
Attia <i>et al.</i> [11]	36 x 36	5.1	9.6
Proposed Antenna	28 x 16	29.8	22

## 4. Conclusion

In this paper, the performance of SRR based tapered patch antenna along with defected ground structure is analyzed and studied. The proposed antenna operates over three different frequencies viz., 3.31 GHz, 6.50 GHz and 12.01 GHz with fractional bandwidths of 19.6%, 8.6% and 29.8%. The maximum return loss of -57 dB has been achieved over 10.36-13.95 GHz at 12.01 GHz. The maximum realized gain of 22 dB is obtained at 12.07 GHz. The antenna exhibits endfire radiation pattern in its far-field characteristics. It is applicable in defense and military applications, satellite communication, several medical applications like cancerous cell detection, tumor and microimaging in medical analysis for determination of radio waves and also in many communication fields.

## 5. References

1. G. V. Eleftheriades and K. G. Balmain, Eds., *Negative Refraction Metamaterials: Fundamental Principles and*

*Applications*, 2005, Hoboken-Piscataway, NJ: Wiley-IEEE Press.

2. C. Caloz, T. Itoh, *Electromagnetic Metamaterials: Transmission Line Theory and Microwave Applications*, 2006 John Wiley & Sons, Inc.

3. Nasimuddin, Z. N. Chen, X. Qing, "Substrate Integrated Metamaterial-Based Leaky-Wave Antenna with Improved Boresight Radiation Bandwidth", *IEEE Transaction Antennas and Propagation*, **61**, 7, July 2013, pp.3451-3457, doi:10.1109/TAP.2013.2256094.

4. Y. D. Dong and T. Itoh "Composite right/left-handed substrate integrated waveguide and half mode substrate integrated waveguide leaky-wave structures", *IEEE Transaction Antennas Propagation*, **59**, 3, March 2011, pp.767 -775, doi:10.1109/TAP.2010.2103025.

5. Otto, S. Rennings, A. Caloz, C. Waldow, P. Itoh, T, "Composite Right/Left-Handed Lambda-Resonator Ring Antenna for Dual-Frequency Operation", *IEEE Antenna and propagation society international symposium*, 2005, pp 684-687, doi:10.1109/APS.2005.1551413.

6. S. Naoui, L. Latrach, A. Gharsallah, "Equivalent Circuit Model for Double Split Ring Resonators", *International Journal*, **11**, 1, Jan. 2016, pp.1-4, doi:10.1002/mop.28393.

7. W.W. Choi, K. F. Chang, C. C. Leong, P. Cheong and K. W. Tam "Design and analysis of defected ground structure transformer for dual-band antenna", *The Journal of Engineering*, October 2014, pp. 612-617, doi:10.1049/joe.2014.0275

8. J. Joubert, J. C. Vardaxoglou, W. G. Whittow, and J. W. Odendaal, "CPW-fed cavity-backed slot radiator loaded with an AMC reflector," *IEEE Transaction Antennas Propagation*, **60**, 2, Feb. 2012, pp. 735-742, doi: 10.1109/TAP.2011.2173152.

9. C. Deng, Y. Li, Z. Zhang, and Z. Feng, "A wideband isotropic radiated planar antenna using sequential rotated L-shaped monopoles", *IEEE Transaction Antennas Propagation*, **62**, 3, March 2014, pp. 1461-1464, doi:10.1109/TAP.2013.2293787.

10. Y.-M. Pan, K. W. Leung, and K. Lu, "Compact quasi-isotropic dielectric resonator antenna with small ground plane", *IEEE Transaction Antennas Propagation*, **62**, 2, Feb. 2014, pp. 577-585, doi:10.1109/TAP.2013.2292082.

11. H. Attia, L. Yousefi and O. M. Ramahi, "Analytical model for calculating the radiation field of microstrip antennas with artificial magnetic superstrates: Theory and experiment", *IEEE Transaction Antennas Propagation*, **59**, 5, May 2011, pp. 1438-1445, doi: 10.1109/TAP.2011.2122295.